

# “An Analysis Of Effect Of Variation In Reynolds Number On Aerodynamic Damping Of Aerofoil Blade With Feasibility Of Active Damping Method”

Narendra D. Khairnar<sup>1</sup>, Dr. Avinash D. Bagul<sup>2</sup>, Dr. Sanjay P. Shekhawat<sup>3</sup>

<sup>1</sup>Research Scholar, Deptt. of Mech. Engg., Gangamai CoE, Nagaon, KBC North Maharashtra University, Jalgaon (India), [narendrakhairnar2020@gmail.com](mailto:narendrakhairnar2020@gmail.com)

<sup>2</sup>Associate Professor, Deptt. of Mech. Engg., Gangamai CoE, Nagaon, KBC North Maharashtra University, Jalgaon (India), [avinashbagul58@gmail.com](mailto:avinashbagul58@gmail.com)

<sup>3</sup>Professor, Deptt. of Mech. Engg., G H Raisoni CoE&M Jalgaon, KBC North Maharashtra University, Jalgaon (India), [sanjay.shekhawat@raisoni.net](mailto:sanjay.shekhawat@raisoni.net)

Aerodynamic damping decreases with low Reynolds, while it increases higher value. With numerical simulation and experimental techniques are applied to analyse how the Reynolds number affects a vibrating air foil blade. Low Reynolds range is applied to pitching air foil blade. Steady and unsteady laminar separation takes place simultaneous over the air foil blades which indicates that, unsteady laminar separation takes place during the transition process following the separated boundary layers separation in an unsteady flow. In the vibrating condition, the rise in Reynolds number results in reattachment and uneven laminar separation. For  $Re = 4 \times 10^5$  at lower Reynolds number pressure on the surface is substantially maximum at the pressure differential out of both aero foil surfaces is minimum as the Reynolds number is increased. The pressure distribution is comparable for  $Re = 2 \times 10^6$  and  $Re = 4 \times 10^6$ . Therefore, it is also studied that using Finite Element Simulation method, number of active and passive techniques have been used to analyses the flow over different aerofoil blades which equipped with piezoelectric actuator. It constitutes relationship in ANSYS and places the piezoelectric actuator in the optimise location. Piezoelectric actuator is attached to the front side of the blade and it is expected that both will adhere perfectly. The attempt is made to analyse for natural frequency and mode shape determination. Active control system provides proactive rather than merely damping response.

**Keywords:** Reynolds number, Aerodynamic Damping Aerofoil, Blade shapes, PZT, natural frequency, FEA.

## I. Introduction

Over the recent time span, wind turbine blade lengths have increased in order to more efficiently capture wind energy. Modern wind turbine blades are designed to be incredibly long and flexible while weighing less, which results in reduced damping values. When the structure is vibrated by external stresses, this causes instabilities. [1]. so, in order to improve

structural damping, most of the investigations have focused on the blade's structural stability [2]. Blades geometry also requires aerodynamic dampening in addition to structural damping. Blade vibration caused to aerodynamic excitation is either suppress or undammed by aerodynamic damping effect. [3]. an energy is induced in the blade structure by the aero foil's behavior, which causes the blade to vibrate. Blade vibration is increased by external aerodynamic forces, if the blades lack adequate structural and aerodynamic damping elements. [4-7]. Blade vibrates at a frequency that is near to blade structure's inherent frequencies, when there is flutter. [8]. Turbine blades and aerodynamic aircraft propellers are unavoidably experience an unstable flow while in flight. Furthermore, an uneven flow has a detrimental impact on an aerodynamic load because it causes vibration. There are two types of unsteady flow pro-stall and pre-stall. After point of separation, eventually approaches a fore-front vortex, invicid- viscous interaction at high angle of attack has important role in the condition of dynamic stall. [9], However, inside stall unsteady boundary layer is dominated by the temporary delay is composed of both boundary layer convection and circulation lag. [10-13] flow prior to the separation of the boundary layer is directly impacted by the time delay. A laminar separation that is unstable is an extremely complex with unclear process for unsteady flow in the low Reynolds number in region. [14] It is observed that in case of unstable flow, opposite direction of flow occurs in absence of boundary layer breakaway either breakdown. In other words, the boundary layer may not break down even, if the reverse flow takes place. Additionally, unstable laminar separation does not occur at the point of zero shear stress.[15].

Actuator (Transducer) in any form acts as smart material and responds to their surrounding very quickly. It stimuli by processing, transmitting, or receiving signal and generating a desirable effect which includes a signal that the material are acting upon it. [16] As a smart material, piezoelectric material has been widely employed as vibration control sensors and actuators due to their excellent properties like portability, large bandwidths, effective energy conversion, simple integration technique.[17]. The application of piezoelectric material in the development of damping or control equipment's provides a promising method for reducing the vibration of turbo machinery blades. [18] Both active and passive methods that use piezoelectric transducers that have been tested experimentally and computationally are used to reduce vibrations in Turbomachinery blades. [19] Vibration suppression of an aerofoil in a compressor stator row is investigated experimentally. Zirconate Titanate array of lead. Piezoelectric components made of PZT are attached to the thin low aspect ratio. Tuned Electrical circuits are coupled to Aerofoils. There is resonant chord wise excitation of the airfoil. The results of experiments show that shunted piezoelectric have important bending mode. Dampening capabilities and may be a useful for reducing or eliminating gas emissions, vibration caused by the passage of compressor blades and turbines blades.[20], [21], [22] Studied several methods for lowering mistuned bladed disk vibration. A piezoelectric patch is attached to each beam and is connected to an electrical network effectively suppresses vibration by establishing a new electro-mechanical energy channel that maintains energy transmission throughout the structure.[23], the use of a piezoelectric patch on the top of a reduced blade model to reduce vibration the size along placement of piezo component is calculated using a Euler's- Bernoulli beam model and a finite element method is provided [24].

## II. Background

An aerodynamic performance of WTS is reduced at low Reynolds number due to the prevalence of boundary-layer separation and stall over the aerofoil blades. Vibration can effectively control the development of dynamic stall and improve performance by taking into account the additional energy that the turbine adds to the flow. [25]. Passive Vibration method like artificial jet actuators [26], along with vortex generators [27] have been utilized in recent years to regulate the stall of wind turbine blades. [28] Presents the expanded version of the local piston theory to accommodate the arbitrary motion of airfoils.[29] the NACA 4412 WT's blades flow detachment and separated shear layer are controlled by partially deformable membrane at comparatively lower RE values. According to the experiments, using the membrane control equipment reduces the generation of LSB. In Addition, the lift coefficient has been enhanced. [30] Evaluated the effect of tip in controlling the stall and separation point over a wind turbine's NACA9415 aerofoil blades using computational fluid dynamics (CFD). The blade tip gap, which significantly improves the power parameter taking into account the blades vibration induced deformation is one of the most often used active control techniques. [31]. Energy is added to the near wall to fluid stay to stay more affixed to blade surface to the dynamic's oscillation surface. It is based on Reynolds number and angle of attack.[32] Active oscillation of the E387 airfoil are simulated numerically in two dimensions at Reynolds number of 30000. Formation of boundary layer on the blade surface is more accurately calculated using DNS, because of the high computations costs, they limited their calculations to RNS model and came to the conclusion that, although the lift coefficient is significantly enhanced, the laminar separation across the different angle of attack (AOA) [33], The authors change the camber to take into account active vibrations over the NACA-4415 Aerofoils suction side. In order to determine the flow separation for RE values & AoAs, they used a visualization approach. They found that, in contrast to the fixed WT blade, the separated regions on the oscillating shank. [34] The Separation control over a NACA-4412 blade at low Reynolds numbers is statistically examined. Concluded that the separation area above the blade is much reduced by the actuation. [35]

### **III. Literature Review.**

**Shengyi Wang, et al (2010)** examines the dynamic stall phenomena at low Reynolds numbers related to unsteady flow around the NACA 0012 Aerofoil using a 2D computational approach. Using computational Fluid Dynamics (CFD), two sets of oscillating patterns with varying frequencies, mean oscillating angles, and amplitudes are numerically simulated. The outcomes are then verified against the matching published experimental data. The experimentally obtained vortex shedding predominant flow structure is well captured by the CFD prediction, and findings quantitatively correlate well with experimental data exception of extremely high angle of attack of blades [36].

**F. A. Najar, et al (2013)** as per analysis of blade, four types of aerodynamics models that are applied to aerodynamic performance of blades, the actuator line model, lifting panel and vortex model, computational fluid dynamics (CFD), model, and the blade momentum (BEM) model. The CFD model is applied to calculate the aerodynamics effect on the blade air foil, while the

critical Reynolds number and constant wind speed are studied while conducting analysis under various turbulence models like Spalart-allamars, K- epsilon, and in turbulent flow. [37]

**A.M. Morad, et al (2015)** they address a method of dampening vibrations in small unmanned aerial (UAV) by using piezoelectric transducers to a genuine propeller blade. The propeller without piezoelectric transducers is first simulated numerically in ANSYS workbench. The findings are then verified by comparing them to experimentally observed model data. Piezoelectric transducers are passively applied to propellers. 1<sup>st</sup> mode high modal strain region in order to reduce vibration. A tool ACT (Application Customization Toolkit, piezo extension) and it is used to model piezoelectric transducers.[38]

**Kemal Koca et al (2017)** at low Reynolds numbers, they show a connection between the wind turbine blades wakes and suction surface vortex shedding and aerodynamics characteristics. The NACA -4412 airfoils force is measured at various Reynolds number and attack angle, while long bubbles can generate noise and vibration at the wind turbine blade, it should be more widely recognized and removed in order to improve the turbines aerodynamics performance and energy efficiency. [39]

**H. Khairnar, G. B. Patil, et al**-Reynolds averaged shear stress transfer turbulence model combined with Navier Stokes flow simulation captures complex flow phenomena in wind turbine blades with flat back and non-flat-back air foil. Three-dimensional computational fluid dynamics (CFD) flow study findings showed that at a particular point of the root region, in spite of the fact that both air foil blades are constructed utilizing blade element momentum theory to provide similar shaft power. [40]

**F. J. Argus, et al (2020)** the laminar-turbulent transition modifies the existence and degree of laminar boundary layer separation, it has a substantial impact on the rotor performance at low Reynolds numbers. The deck are Inco rated into a 3 D flow solver that combines a blade element. Theory model with RANS flow solution. To access rotor performance over crucial amplification factor and Reynolds number sweeps. Reducing the rotors figure of merit in Hover by around 40 % requires raising the essential implication factor from 3 to 11 for chord-based renolyds number between &  $Re^{3/4} = 2 \times 10^4$ . The significant decline in performance at low Reynolds number is due to laminar separation. The conventional air foil rotors are strongly influenced by the operating condition for Reynolds number below  $2 \times 10^4$ . [41]

**Ping Hu, et al (2020)** Using the dynamic mode decomposition approach the vortex-induced vibration of a forced oscillating examined. With frequency ratio between 0.8- and 1.2, the airfoil will become unstable condition prior to existing the locked in region for a series of forced vibration calculations with constant amplitude. Parameters of energy exchange on the airfoil surface are primarily influenced by a smooth phase shift between the vibrations induced aerodynamic force and the airfoil motion. Decomposition is used in the final dynamic mode to find various flow characteristics in the flow field that show the vortex vibration.[42]

**Ajay Veludurthi et al (2020)** an examination of the small model with harmonic characteristics of turbine blade from NACA 63415 series. The sandwich structure composite blade is made of GERP and epoxy. It has stiffeners made from univinyll hard foams in various alignments.

The finite element approach used with ANSYS 18.1 Software to do modal & harmonic analysis of various types of blades such as solid, hollow and rectangular alignment blades. It provides the natural frequencies, amplitudes, and mode shapes. Using a vibration test rig with specifically made fixtures, experimental examination is carried out. The blades reactions to various stresses and frequencies are analyzed using vibration, which provides workable research to determine the optimal blade construction. To determine the amplitude at various frequencies, harmonic analysis is also performed for various materials. The analysis findings give a guide for enhancing the blades material qualities and structure.[43]

**K. Koca, et al (2021)** The LSB formations mapping on to a turbine blade along various air foils shapes with vibrational effects are investigated experimentally. Aerodynamic force measurement's using an external force balancing system, quasi-wall shear stress measurements using hot film sensor, comprehensive instantaneous and time visualizations. Findings from the smoke-wire and voltage signals from the sensor of hot film are found to be strongly correlated. The magnitude of variations began to rise within the LSB, particularly near the region. LSB formed as a result of the foils varying thickness and camber, which caused the aerodynamics forces to change over the time. Such as vibrations at the blades edges and flaps, which results in stochastic loads and shorten turbine blade lifespan. [44]

**S. W. Naung, et al (2021)** they analyse a WT blades air foils aerodynamic and aeromechanical performances using a highly effective numerical using a highly effective numerical approach providing a thorough understanding of the unsteady flow behaviour under operating situations. An air foils surface pressure changes at different attack angles are measured experimentally. Then using a frequency-domain approach. Flow field characteristics are using the aeromechanical models of WT blade aerofoils for variety of parameters, such as Reynolds numbers and angle of attack are determined. For precise results the frequency and time domain solutions are accurately compared [45].

**Prahallada Jutur, et al (2022)** with low Reynolds numbers and low frequencies ( $k = 0.1$ ) and  $Re = 50000$ , the stall vibration of linear cascade experiencing significant amplitude oscillations (10% of chord) is experimentally investigated. In order to depict weightless, average and deep stall position in cascade, three blade incidence situations are examined. When the blades in the cascade are permitted to exhibit large amplitudes heaving oscillations at the specified decreased frequency ( $k$ ) frequency ( $k$ ) between phase angle ( $\Theta$ ) measurements of the flow field are made using particle image Velocimetry (PIV) and transmission of energy is measured simultaneously using load cell. In view of blade displacement, the findings indicate that the shear layer phase is near the unsteady force phase ( $\Phi$ ) which is helpful. An experimental study is conducted of stall flutter of a linear cascade with large amplitude exhibits oscillations (10% of chord) for low Reynolds numbers  $Re$  and a low reduced frequencies  $k \leq 0.1$  and at low  $Re = 50000$ . [46]

#### **IV. Vibration Analysis of a Aerofoil Blade.**

Alaa M. Morad et al. Conducted experimental work along with software analysis, in which active vibration control using piezoelectric sensors and actuators. Conducting tests is essential for model calibration and validation of numerical models. The initial set of testing is performed with a tiny hammer, whereas the subsequent series utilizes a shaker applied to one of the propeller blades tips.[48]



Fig.-1. Blade propeller in real shape. [48-1]

#### a. Modal test of blade using hammer.

A series of experiments is run on fixed propeller from the hub, simulated by a small hammer. Three ceramic shear piezoelectric accelerometers. PCB piezo electronics are utilized hammer in manufacturing. The utilised hammer is the Integrated Circuit Piezoelectric impulse force test small impact hammer technique. The dynamic characteristics of a structure are delineated by its inherent frequencies and accompanying vibration modes. The dynamic characteristics of a structure are defined by its inherent frequencies and accompanying vibration modes.

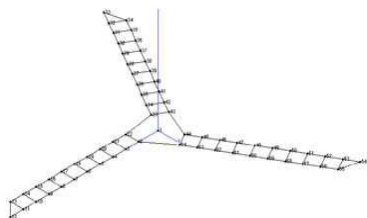


Fig. 2. Blade Shape in LMS program using 64 points. [48-3]

An accelerometer placed to the tip of a propeller blade. This modal testing approach is referred as frequency Response Function (FRF) method, which concurrently determines input (FRF) method, which concurrently determines input excitation and output response. The frequency Response function is illustrated in the fig.-3, while the proper mode forms are presented below,

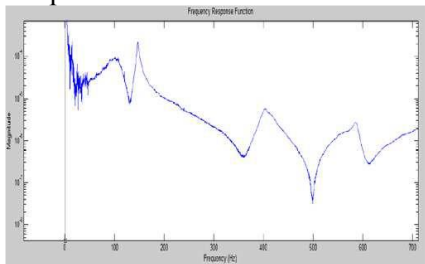
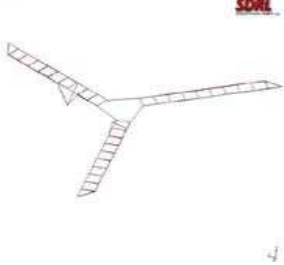
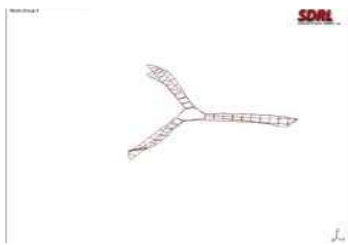


Fig.3. Frequency Response Function FRF of propeller. [48-4]



Mode 1.



Mode 6.

Fig.4. -Experimental propeller mode shapes using hammer. [48-5]

#### **b. Modal Analysis Using Shaker System.**

Employing a shaker mechanism for modal testing to conduct the prior modal testing conducted with a hammer. The LMS SCADAS laboratory comprise a PC, SCADAS -III data gathering system, signal amplifier, shaker, force transducer and 21 accelerometers are applied. Propeller is secured at the hub and connected to a shaker at the tip of one blade, which is vibrated correspondingly. The shakers power amplifier delivers requisite power levels over the operational frequency spectrum, enabling the shaker to provide a regulated force output.

When modes natural frequency is reached or close to it, the mode shape of the response will tend to rule the general shape of the waves in structure. Frequency Response function technique is used for this kind of modal stability testing. The propeller is tested for modal stability at frequencies range from 0 to 1000 Hz. The frequency Response Function and the (FRF) and the propeller mode forms are studied. The natural frequencies response that go with the different mode numbers for both the hammer and shaker studies as shown in Table-1.

#### **b. Simulations in Ansys (FEA) Software.**

The propeller size is measured, then designed using Auto CAD application software and its shape is loaded into 3-D ANSYS-15 workstation. The propeller is initially modelled and meshed using 13611 mesh elements and 25374 nodes in ANSYS- structure before performing modal analysis in ANSYS workbench, it is important to make sure cell- based smoothed finite element method is reliable and produces correct results as the number of degrees of increases,



mesh convergence analysis is carried out. The propeller boundary conditions and the material characteristics are used, while calculations are done with selected modal analysis.

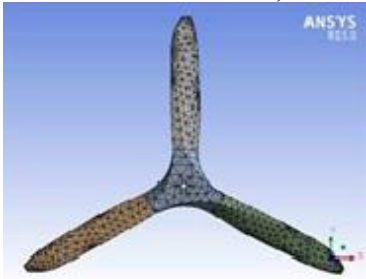
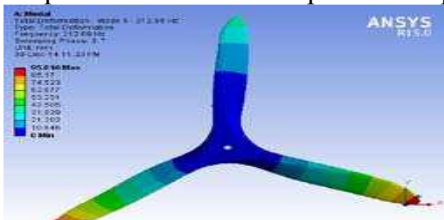


Fig.6. Mesh configuration of the propeller in ANSYS. [48-11]

**c. Finite Element Analysis without Transducer.**

Determination of the mode shapes along with natural frequency, Finite Element Analysis of the propeller without piezoelectric transducer is built up and examined. At zero rotation speed, the propeller mode shapes and modal displacement contours are displayed as shown in fig.-7 displays the comparison of the results of the numerical simulations in ANSYS for natural frequencies and mode shapes with experimental data.



Mode 1.

Mode 6.

Fig.7. Modal Displacement contour without Piezoelectric Transducers [48-12]

Mode shape	Hammer (Hz)	Shaker (Hz)	ANSYS (Hz)
1	46.123	45.567	45.173
2	68.451	68.952	67.479
3	71.123	71.321	71.547
4	150.645	184.36	185.271
5	185.213	184.36	185.274
6	210.94	211.63	212.693

Corresponding elastic strain for the first mode form is displayed in fig.-8 where the piezoelectric transducers are positioned. A complete adhesive connection between transducers and blades is expected when piezoelectric transducers are glued to the front side of the blade.



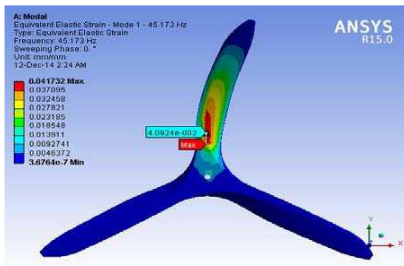


Fig.8. Maximum Strain area from modal analysis for the first mode shape. [48-11]

## V. Discussions & Future Work

At every Reynolds number a significant variation in the unstable pressure differential is seen along the aerofoil. Coefficient of unstable pressure amplitude is progressively increases from 0.5 and then gradually decreases. This suggest that at lower Reynolds number, there is a significant variation of pressure variation along the aerofoils chord. Vibrating aerofoil with a reduced Reynolds number intensifies flow unsteadiness, leading to flow separation and the creation of vortices along the aerofoil. An increasing design of unstable pressure and fluctuating behaviour are seen when the Reynolds number is raised to  $8 \times 10^5$ . This unstable pressure distribution behaviour along the chord is further decreased by raising the Reynolds number.

**I.** At  $Re = 4 \times 10^5$  surface pressure is likewise significantly maximum than for lower Reynolds Number. Now between these two aerofoil surfaces is lowered, when Reynolds number is increased. The pressure distribution is comparable for  $Re = 2 \times 10^6$  and  $Re = 4 \times 10^6$  at lower Reynolds numbers, and pressure differential is larger.

**II.** It is possible to see Reynolds numbers impact on the flow field surrounding aerofoil using velocity distributions. Higher Reynolds number are associated with less flow separation, whereas lower Reynolds numbers are associated with more unsteadiness. Trailing edge vortex formation found similar to Karman Vortex for  $4 \times 10^5$ . At  $Re = 8 \times 10^5$ , the vortex frequency is less important, but laminar vortex shedding generation and the laminar to turbulent change is visible clearly along trailing edge. Since flow becomes significantly more powerful at higher Re values, eventually reduce detached shear layers and recirculation, behavior of vortex shedding is virtually not identified at  $Re = 4 \times 10^6$ . At higher Reynolds number turbulent boundary layer is more stable. Aerodynamic damping values computed to examine the impact of varying Reynolds numbers for aeroelastic performance of aerofoil, in line with earlier analysis for various AoAs.

**III.** Both frequency & time domain techniques are used to compute aerodynamic damping values. Frequency domain technique results closely match ones from the conventional domain method. Aerodynamic damping is comparatively low  $Re = 4 \times 10^5$  and  $2 \times 10^6$ . It progressively increases as the Reynolds number raised  $2 \times 10^6$ . This in spite of the fact that all the Reynolds

number have positive aerodynamic damping values. Aerodynamic damping at  $Re = 4 \times 10^6$  is 56% and 88 % greater than at  $Re = 2 \times 10^6$  and  $Re = 4 \times 10^5$  respectively.

**IV.** At decreasing Reynolds number, vortex production causes the flow to become more unsteady. The blade is subject to aerodynamics forces due to the creation of vortices and variation in pressure. Blade failure result from blade vibration when the blades absorb energy from the flow. If aerodynamic dampening is insufficient to reduce the vibration. For this reason, selected the right operating conditions including Reynolds Number, which is crucial when designing blades for offshore wind turbines.

**V.** Active damping methods is evolved to be a promising method to damp the vibration for low Rey molds number value. An Aerodynamic damping is significantly increasing above certain level of Reynolds of airflow.

## **VI. Conclusion.**

Increasing Reynolds number reduces the flow separation. According to estimation of aerodynamic damping at different Reynolds numbers, stronger flow unsteadiness at lower Re numbers results in comparatively low aerodynamic damping, which has an impact on blade stability. As the Reynolds increases, the aerodynamic damping increases as well, reaching its maximum at  $Re = 4 \times 10^6$ . If aerodynamic Damping is insufficient to dampen level of vibration, blades vibration may cause flutter instability as it accumulates energy from the flow. As a result, the design process greatly depends on the choice of operating conditions, including Reynolds number. Frequency and time domain solution approach is used most often to analyses. Both approaches yield very good results, accuracy in the frequency domain solution is guaranteed. Traditional time domain approach takes 90% longer to solve than frequency domain method. Also, numerical simulation and experimental modal analysis without piezoelectric transducers match quite well, with a variation of around 1% to 2%. Natural frequencies are increased when piezoelectric transducer is used, according to a study of natural frequencies with and without them. Furthermore, employing piezoelectric transducer lowers the amplitudes for FRF in the first three mode shapes as well as the maximum value of the elastic strain for the first mode. It is determined that employing piezoelectric transducers for non-rotating propeller reduces the maximum value of equivalent elastic strain by 24.6 %.

## **VI. Acknowledgment.**

Thankful to owners of experimental work Alaa M. Morad, Aly Elzahaby, S. Abdallah, M. Kamel and Mohamed K. Khalil for their valuable contribution.

## **REFERENCES**

- [1] M. M., Behzad, M., Haddadpour, H., & Moradi, (2017) "Aeroelastic analysis of a rotating wind turbine blade using a geometrically exact formulation", *Nonlinear Dynamics*, 89(4), 2367-2392.
- [2] Chaviaropoulos, P. K., Politis, E. S., Lekou, D. J., Sørensen, N. N., Hansen, M. H., Bulder, B. H., Winkelaar, D., Lindenburg, C., Saravanos, D. A., Philippidis, T. P., Galiotis, C., Hansen, M. O. L., and Kossivas, T., (2006) "Enhancing the damping of wind turbine rotor blades", the DAMPBLADE project, *Wind Energy*, 9(1-2), 2006, 163-177.
- [3] Ramdenec, D., Ilinca, A., and Minea, I. S., (2012) "Aero elasticity of Wind Turbines Blades Using Numerical Simulation", *Advances in Wind Power*, 2012, 87-120.

- [4] Hansen, M. H., (2003) "Improved Modal Dynamics of Wind Turbines to Avoid Stall-induced Vibrations", *Wind Energy*, 6(2), 2003, 179-195.
- [5] Hansen, M. H., (2004) "Aeroelastic stability analysis of wind turbines using an eigenvalue approach", *Wind Energy*, 7(2), 2004, 133-143.
- [6] Hansen, M. H., (2003) "Aeroelastic eigenvalue analysis of three-bladed wind turbines", 2003, <http://hdl.handle.net/20.500.11881/375>
- [7] Thomsen, K., Petersen, J. T., Nim, E., Øye, S., and Petersen, B., (2000) "A Method for Determination of Damping for Edgewise Blade Vibrations", *Wind Energy* 3(4), 2000, 233-246.
- [8] Patil, S., Zori, L., Galpin, P., Morales, J., and Godin, P., () "Investigation of Time/Frequency Domain CFD Methods to Predict Turbomachinery Blade Aerodynamic Damping".
- [9] Lobitz, D. W., (2004) "Aeroelastic stability predictions for a MW-sized blade", *Wind Energy*, 7(3), 2004, 211-224.
- [10] Lobitz, D. W. (2005) "Parameter Sensitivities Affecting Flutter Speed of a MW-Sized Blade", *Journal of Solar Energy Engineering*, 127(4), 538-543.
- [11] Dezvareh, R., (2019) "Evaluation of turbulence on the dynamics of monopile offshore wind turbine under the wave and wind excitations", *Journal of Applied and Computational Mechanics*, 5(4), 2019, 704-716.
- [12] Pierella, F., Krogstad, Sætran, (2014) "Blind Test 2 calculations for two in-line model wind turbines where the downstream turbine operates at various rotational speeds", *Renewable Energy*, 70, 2014, 62-77.
- [13] Krogstad, P.-Å., Sætran, L., and Adaramola, M. S., (2015) "Blind Test 3" calculations of the performance and wake development behind two in-line and offset model wind turbines, *Journal of Fluids and Structures*", 52, 2015, 65-80.
- [14] Wang, L., Liu, X., and Kolios, A., (2016) "State of the art in the aeroelasticity of wind turbine blades: Aeroelastic modelling", *Renewable and Sustainable Energy Reviews*, 64, 2016, 195-210.
- [15] Kaya, M. N., Kose, F., Ingham, D., Ma, L., and Pourkashanian, M., (2018) Aerodynamic performance of a horizontal axis wind turbine with forward and backward swept blades, *Journal of Wind Engineering and Industrial Aerodynamics*, 176, 2018, 166-173.
- [16] J.A. Harvey, *Mechanical Engineers' (2006) "Handbook: Materials and Mechanical Design."* vol. 1, Third Edition: Wiley, 2006.
- [17] B. Zhou, F. Thouverez & D. Lenoir (2012) "A nonlinear vibration absorber based on nonlinear shunted piezoelectrics," *ASME* vol. GT2012-69322, 2012.
- [18] S. Livet, M. Berthillier, M. Collet and J. Cote (2007) "Numerical and experimental optimized shunted piezoelectric circuit for turbomachinery blades," presented at the 12th IFToMM World Congress, Besancon, 2007
- [19] C. Cross, and S. Fleeter, (2002) "Shunted Piezoelectrics for Passive Control of Turbomachine Blading Flow-Induced Vibrations," *Smart Materials and Structures* vol. II , p. 239, 2002.
- [20] H. Yu, K. Wang and J. Zhang (2006) "Piezoelectric networking with enhanced electromechanical coupling for vibration delocalization of mistuned periodic structures—theory and experiment," *Journal of Sound and Vibration*, vol. 295 (1-2), pp. 246–265., 2006
- [21] H. Yu, and K.W. Wang, (2007) "Piezoelectric networks for vibration suppression of mistuned bladed disks," *Journal of Vibration and Acoustics*, vol. 129 (5), pp. 559–566., 2007.
- [22] H. Yu, and K.W. Wang, (2009) "Vibration suppression of mistuned coupled blade-disk systems using piezoelectric circuitry network," *Journal of Vibration and Acoustics*, vol. 131(2), p. 021008, 2009.
- [23] S. Livet, M. Berthillier, M. Collet and J. Cote (2007) "Numerical and experimental optimized shunted piezoelectric circuit for turbomachinery blades," presented at the 12th IFToMM World Congress, Besancon, 2007

- [24] S. Livet, M. Collet, M. Berthillier, P. Jean, and J.M. Cote, (2008) "Turbomachinery Blades Damping Thanks to Optimized Shunted Piezoelectric Circuits," in *Active and Passive Smart Structures and Integrated Systems*, 2008. [25] A. Choudhry, M. Arjomandi, R. Kelso Methods to control dynamic stall for wind turbine applications *Renew. Energy*, 86(2016), pp. 26-37
- [26] M. Amitay, D.R. Smith, V. Kibens, D.E. Parekh, A. Glezer Aerodynamic flow control over an unconventional airfoil using synthetic jet actuators *AIAA J.*, 39(2001), pp. 361-370
- [27] L. Gao, H. Zhang, Y. Liu, S. Han (2015) Effects of vortex generators on a blunt trailing-edge air foil for wind turbines" *RE*, 76, pp. 303-311
- [28] M.-C. Meijer, L. Dala Generalized formulation and review of piston theory for airfoils *AIAA J.*, 54(2016), pp. 17-27
- [29] H.H. Açikel, M.S.(2018) "Control of laminar separation bubble over wind turbine airfoil using partial flexibility on suction surface *Energy*", 165, pp. 176-190.
- [30] A. Saleem, M.-H. Kim Effect of rotor tip clearance on the aerodynamic performance of an aerofoil-based ducted wind turbine *Energy Convers. Manag.*, 201(2019), Article 112186.
- [31] I.S. Hwang, S.Y. Min, I.O. Jeong, Y.H. Lee, S.J. Kim Efficiency improvement of a new vertical axis wind turbine by individual active control of blademotion, *Smart Structures and Materials 2006: Smart Structures and Integrated Systems International Society for Optics and Photonics* (2006), p. 617311.
- [32] J. Lei, J. Zhang, J. Niu Effect of active oscillation of local surface on the performance of low Reynolds number airfoil *Aero. Sci. Technol.*, 99(2020), Article 105774.
- [33] D. Munday, J. Jacob Active control of separation on a wing with oscillating camber *J. Aircraft*, 39(2002), pp. 187-189
- [34] V. Katam, R. LeBeau, J. Jacob Simulation of separation control on a morphing wing with conformal camber 35th *AIAA Fluid Dynamics Conference and Exhibit* (2005), p. 4880.
- [35] H. Jokar, M. Mahzoon, R. Vatankhah Dynamic modeling and free vibration analysis of horizontal axis wind turbine blades in the flap-wise direction *Renew. Energy*, 146(2020), pp. 1818-1832.
- [36] Shengyi Wang Derek B. Ingham, Lin M, Mohamed Pourkashanian Zhi Tao (2010), "Numerical investigations on dynamic stall of low Reynolds number flow around oscillating aerofoils, *ScienceDirect, Computers & Fluids*, 39 (2010) 1529–1541,
- [37] Zhifeng Yao, Fujun Wang, Matthieu Dreyer, Mohamed Farhat, (2014), "Effect of trailing edge shape on hydrodynamic damping for a hydrofoil", *Science Direct*, [p://dx.doi.org/10.1016/j.jfluidstructs.2014.09.003](https://doi.org/10.1016/j.jfluidstructs.2014.09.003), 22 October 2014
- [38] A. M. Morad, A. Elaraby, S. Abdallah, M. Kamel & M. K. Khalil, (2015) "Application of Piezoelectric Materials for Aircraft Propeller Blades Vibration Damping" *International Journal of Scientific & Engineering Research*, Volume 6, Issue 8, August-2015 ISSN 2229-5518
- [39] Kemal Koca, Mustafa Serdar Genç, Halil Hakan Açikel, Mucahit Çağdaş, (2015) "Tuna Murat Bodur, Identification of Flow Phenomena over NACA 4412 Wind Turbine Airfoil at Low Reynolds Numbers and Role of Laminar Separation Bubble on Flow Evolution", *Energy* (2017), doi: 10.1016/j.energy.2017.12.045.
- [40] H. Khairnar, G. B. Patil, S. Ghugare, B. More, S. Ushkewar and M. Mali, "Load Frequency Control using PID Controller," 2024 2nd International Conference on Sustainable Computing and Smart Systems (ICSCSS), Coimbatore, India, 2024, pp. 190-195, doi: 10.1109/ICSCSS60660.2024.10625307.
- [41] Finbar J. Argus Geoffrey A. Ament2 Witold J. F. Koning, (2020) "The Influence of Laminar-Turbulent Transition on Rotor Performance at Low Reynolds Numbers", *VFS Aeromechanics for Advanced Vertical Flight Technical Meeting*, San Jose, CA, January 21–23, 2020.
- [42] Ping Hu, Chong Sun, Xiaocheng Zhu, & Zhaohui Du (2020) "Investigations on vortex-induced vibration of a wind turbine airfoil at a high angle of attack via modal analysis", *J. Renewable Sustainable Energy* 13, 033306 (2021); <https://doi.org/10.1063/5.0040509>.

- [43] Ajay Veludurthi & V. Bolleddu (2020) "Experimental Study on Modal and Harmonic Analysis of Small Wind Turbine Blades Using NACA 63-415 Aerofoil Cross-Section", *Energy Engineering* DOI: 10.32604/EE.010666, EE, 2020, vol.117, no.2.
- [44] Kemal Koca, Mustafa Serdar, Ramazan Özkan (2021) "Mapping of laminar separation bubble and bubble-induced vibrations over a turbine blade at low Reynolds numbers", <https://doi.org/10.1016/j.oceaneng.2021.109867>, *Ocean Engineering* Volume 239, 1 November 2021, 109867.
- [45] Shine Win Naung, Mahdi Erfanian Nakhchi, Mohammad Rahmati (2021) "An Experimental and Numerical Study on the Aerodynamic Performance of Vibrating Wind Turbine Blade with Frequency-Domain Method", DOI: 10.22055/JACM.2021.37406.3011, 03 2021. *J. Appl. Comput. Mech.*, 7(3) (2021) 1737-1750.
- [46] P. Jutur, Dipanjan Barman, Raghuraman N. Govardhan (2022), "Low Reynolds number stall flutter of a linear cascade with large amplitudes at low reduced frequencies: Unsteady loads and flow features", <https://doi.org/10.1016/j.jfluidstructs.2021.103490>, Science direct, *Journal of Fluids and Structures* Volume 109, February 2022, 103490.
- [47] M.E. Nakhchi, S. Win Naung, L. Dala, M. Rahmati (2022), "Direct numerical simulations of aerodynamic performance of wind turbine aerofoil by considering the blades active vibrations", <https://doi.org/10.1016/j.renene.2022.04.052>, Science Direct, *Renewable Energy*, Volume 191, May 2022, Pages 669-684.
- [48] Alaa M. Morada, Aly Elzahaby, S. Abdallah, M. Kamel and Mohamed K. Khalile, (2015) "Application of Piezoelectric Materials for Aircraft Propeller Blades Vibration Damping" *International Journal of Scientific & Engineering Research*, Volume 6, Issue 8, August-2015 ISSN 2229-5518.
- [49] G. Rajput, G. B. Patil, B. Patil, D. Sonawane, S. Pendharkar and Y. Patil, "Bidirectional Charger System Design Enabling V2G and G2V Energy Transfer," 2024 Second International Conference on Inventive Computing and Informatics (ICICI), Bangalore, India, 2024, pp. 720-725, doi: 10.1109/ICICI62254.2024.00122.
- [50] Narendra D. Khairnar, Dr. Avinash Bagul, (2024) "Review on Static & Dynamic analysis of aerofoil blade at different aspect of Research Investigation" Vol. 9 No. GHRIEBM (2024): International Conference on "innovation, technology & entrepreneurship ITE 2024.